Interface Stoichiometry Control to Improve Device Performance in ZnO/Cu_2O Heterojunction Solar Cells

Samantha S. Wilson,[1] Jeffrey P. Bosco,[1] Yulia Tolstova,[1] David O. Scanlon,[2] Graeme W. Watson,[3] and Harry A. Atwater[1]

[1]*Watson Laboratory, Beckman Institute and Kavli Nanoscience Institute, California Institute of Technology, 1200 E. California Blvd., Pasadena, California 91125, USA.*

[2]*University College London, Kathleen Lonsdale Materials Chemistry, Department of Chemistry, 20 Gordon Street, London WC1H OAJ, UK.*

[3]*School of Chemistry and CRANN, Trinity College Dublin, College Green, Dublin 2, Ireland.*

Abstract

The interface stoichiometry of cuprous oxide (Cu_2O) prepared by thermal oxidation was controlled by adjusting the O_2 and Zn partial pressures during ZnO sputter deposition and measured by high-resolution X-ray photoelectron spectroscopy of ultrathin (<3 nm) ZnO films on Cu_2O. Current-voltage characteristics of ZnO/Cu_2O heterojunctions under AM1.5 1-sun illumination were collected for three different interfacial compositions: (1) mixed Cu_2O and Cu, (2) stoichiometric Cu_2O, and (3) and mixed Cu_2O and CuO. ZnO/Cu_2O heterojunctions with stoichiometric interfaces achieved open circuit voltages of V_{OC} = 530 ± 4 mV. V_{OC} = 347 ± 30 mV and V_{OC} = 109 ± 11 mV were achieved for devices where the interface contained Cu and CuO, respectively. Thus a stoichiometric interface is essential for achieving a high voltage photovoltaic device. Additionally, valence-band offset measurements indicated the presence of CuO changed the band alignment between Cu_2O and ZnO, which could account for some of the variation in previously reported values.

1. Introduction

Cuprous oxide (Cu_2O) is a promising alternative to traditional thin-film photovoltaic materials (CIGS, CdTe, a-Si, etc.) because of its low materials cost, the abundance of its component elements in the earth's crust,[1] and its uniquely straightforward processing.[2-4] Crystalline wafers of Cu_2O can be fabricated directly by thermal oxidation of Cu foils, making manufacturing high quality photovoltaic materials possible through low-cost processing.[2, 5] Furthermore, Cu_2O has a band gap of 2.1 eV which gives it a detailed balance efficiency of ~20% for a homojunction solar cell and also the potential for an independently connected Cu_2O/Si tandem device with an efficiency of ~43%.[2, 3, 6, 7] It is an intrinsic p-type semiconductor with relatively high absorbance in the visible region above the gap.[2] Finally, minority carrier

diffusion lengths of 10 μm and hole mobilities of up to 100 $cm^2V^{-1}s^{-1}$ have also been reported for Cu_2O made by thermal oxidation.[2, 5, 6, 8]

Despite band gap and minority carrier properties that are favorable for achieving a high energy conversion efficiency, the highest efficiency achieved in a photovoltaic device with a Cu_2O absorber layer is 5.38%.[9] There are several challenges to making a Cu_2O photovoltaic device, including an inability to dope the material,[2, 10] its relatively low chemical stability compared to other oxides,[11] and a lack of suitable heterojunction partners due to an unusually small electron affinity.[12] We have focused on the low chemical stability, namely the fact that Cu_2O is an especially reactive oxide due to its low enthalpy of formation (ΔH_f^o). A comparison of ΔH_f^o values for various metal oxides can be found in Table I. The low value of the heat of formation means Cu_2O will be reduced to Cu when in contact with nearly any elemental material. Cu forms a low barrier Schottky diode with Cu_2O, thus the presence of interfacial Cu lowers the photovoltaic cell's built-in voltage. The effect of interfacial Cu on device performance has been well characterized for Cu_2O Schottky devices.[2, 13] However Cu is not the only species that may reactively form at the interface as Cu has another stable oxide, cupric oxide (CuO).[14] The effect of interfacial CuO has not been studied explicitly in Cu_2O heterojunctions, and its specific impact on device performance is unknown.

We have chosen to study the ZnO/Cu_2O interface because it has been the most widely studied Cu_2O based heterostructure, and until recently, the most efficient heterojunction system as well.[2, 3, 15-21] In this manuscript, we describe the controlled modification of ZnO/Cu_2O heterostructures to yield stoichiometric interfaces as well as nonstoichiometric interfaces with Cu and CuO present. We also explored the effects of interface stoichiometry on heterojunction device performance. The bulk phase purity of sputter-deposited ZnO films grown on thermally oxidized Cu foils was determined by X-ray diffraction (XRD). The ZnO/Cu_2O interface stoichiometry and valence-band alignments were explored experimentally by high-resolution X-ray photoelectron spectroscopy (XPS). Finally, in order to quantify the effect of local deviations in interface stoichiometry, ZnO/Cu_2O photovoltaic devices of varying interface composition were tested under AM1.5 1-sun solar illumination.

2. Experimental

The Cu_2O wafers used in these experiments were grown by thermal oxidation of 500 μm copper foils (99.9999%, Alfa Aesar) in a tube furnace. The Cu foils were hung vertically from Cu wires on a quartz substrate holder during oxidation. The Cu substrates were heated to 950 °C under N_2 flow and then oxidized for 24 hours at 1 Torr O_2. This temperature and pressure were chosen because they are within the stability range of the Cu_2O phase in the Cu-O phase diagram.[14] The substrates were then cooled to room temperature under a N_2 flow resulting in ~1 mm thick Cu_2O wafers with a lateral grain size on the order of ~1 mm^2.

Heterostructures for XPS and XRD studies were fabricated by rf magnetron sputter deposition of Zn or ZnO directly onto an untreated Cu_2O surface at room temperature. A compound ZnO target and a pure Zn metal target were used as sputtering sources. Zn or ZnO films were deposited at 100 W substrate power and a sputtering pressure of 5 mTorr. ZnO was sputtered under both a pure Ar atmosphere and a 0.25 mTorr partial pressure of O_2 in Ar. The ZnO sputtered with O_2 was O-rich as indicated by its resistivity (ρ>1000 Ω-cm), while the ZnO sputtered in pure Ar was Zn-rich (ρ~1 Ω-cm). Zn was sputtered only under a pure Ar atmosphere. For XPS samples, the thickness of deposited films ranged from 0.5-10 nm, while 100 nm films were used for XRD.

For photovoltaic device fabrication, each of the three interface types was made by depositing ~2 nm of ZnO or Zn, which were sputtered according to the three conditions outlined above, onto a ~1 mm thick, untreated Cu_2O wafer. An additional 10 nm of ZnO sputtered in Ar was deposited onto all the samples and capped with 50 nm of sputtered Al-doped ZnO (AZO) followed by 100 nm of Sn-doped In_2O_3 (ITO) as a top electrical contact. A thick Au film was deposited on the Cu_2O as a back electrical contact. Device area was approximately 3 mm^2.

X-ray diffraction measurements were performed using a high resolution diffractometer in the ω-2θ geometry. The surface stoichiometry and interface stoichiometry of thin ZnO/Cu_2O samples were measured using a Kratos Ultra XPS system. The Al Kα line (1486.6 eV) was used as a monochromatic X-ray source and the excited photoelectrons were collected by a hemispherical analyzer at 0° from the surface normal. Low-resolution survey spectra were acquired between binding energies (B.E.) of 1–1200 eV. Higher-resolution, detailed scans (detection line width of <0.26 eV), were collected on individual XPS features of interest. The sample chamber was maintained at $<2\times10^{-9}$ Torr. Finally, current density vs. potential (J-V) measurements on the full PV devices were performed under AM1.5 1-sun illumination.

3. Results and Discussion

Figure 1 shows XRD spectra for ZnO/Cu_2O and Zn/Cu_2O heterojunctions deposited according to the three conditions detailed above. The XRD scans show the Cu_2O wafers were phase pure, with no Cu or CuO present through the bulk of the wafer. The data also show some preferential orientation for the (110) and (111) directions. These directions are the most close-packed planes so it is hypothesized that the Cu_2O grains nucleate with this preferential orientation to minimize surface energy. Furthermore both the O-rich ZnO and Zn-rich ZnO were phase pure with no Zn inclusions.

3.1 Determination of ZnO/Cu_2O and Zn/Cu_2O interface stoichiometry by X-ray photoelectron spectroscopy

In order to measure the interface stoichiometry, we performed XPS on thin heterointerfaces. Since XPS is a surface sensitive technique, film thicknesses were constrained to less than the escape depth of the photo-excited electrons (~3 nm). This allowed analysis of the heterojunction without the need for sputter depth profiling, leaving pristine interfaces free of crystalline damage. Figure 2 shows survey XPS spectra of the Zn 2p and Cu 2p regions collected on a series of ZnO/Cu_2O interfaces. Both Zn and Cu peaks were simultaneously observed in the XPS spectra indicating we were indeed effectively probing the ZnO/Cu_2O interface.

XPS is a particularly powerful technique for Cu_2O stoichiometry determination because CuO, Cu_2O and elemental Cu can be differentiated by analyzing high-resolution spectra of the Cu $2p_{3/2}$ (Cu 2p) and Cu Auger (Cu a) peaks.[22] If Cu is bound as CuO, the Cu $2p_{3/2}$ peak shifts to slightly higher binding energy. However this one peak is not sufficient to understand the oxidation state of the Cu at the interface since Cu_2O and elemental Cu have the same Cu $2p_{3/2}$ peak position. Elemental Cu can be differentiated from Cu_2O by looking for peak shifts in the Cu Auger peak. Cu shifts to lower binding energies in the Auger peak while Cu_2O and CuO have the same peak position.

Figure 3 shows the high-resolution XPS spectra for different thicknesses of Cu_2O heterojunctions made with (a) O-rich ZnO, (b) Zn-rich ZnO, or (c) elemental Zn. The XPS spectra for the bare Cu_2O wafer (0.0 nm) shows a shoulder in the Cu 2p peak in all samples, indicating there is CuO on the surface of the wafer. This surface oxide forms when Cu_2O is exposed to atmosphere because CuO is the stable phase of copper oxide at room temperature and pressure.[14] When O-rich ZnO is deposited onto the slightly oxidized Cu_2O surface, the shoulder in the Cu 2p peak continues through all thicknesses of ZnO. This result is expected since O-rich ZnO should have no elemental Zn available to react with the surface of the Cu_2O. Thus by depositing O-rich ZnO directly onto the slightly oxidized Cu_2O surface, we can produce a mixed phase surface with both CuO and Cu_2O.

When Zn-rich ZnO is deposited instead of O-rich ZnO, as shown in figure 3(b), we expect the wafer surface to be reduced due to the availability of elemental Zn. The data shows that as Zn-rich ZnO is deposited onto Cu_2O the shoulder in the Cu 2p peak disappears, indicating that the CuO layer is reduced. Furthermore, analysis of the Cu Auger peak shows no Cu_2O is reduced since no low binding energy peak is present, thus the reaction terminates at the Cu_2O surface. The reaction appears to be highly selective, which could be due to the slightly higher ΔH_f^o of Cu_2O versus CuO. This reaction was also found to be highly reproducible and all deposited thicknesses showed the same trend. Thus depositing Zn-rich ZnO onto a slightly oxidized Cu_2O surface yields a stoichiometric ZnO/Cu_2O interface.

Elemental Cu was formed at the interface by sputtering elemental Zn onto Cu_2O because it was found to be impossible to reduce Cu_2O to Cu by sputtering ZnO alone. This is probably due to

the low thermodynamic driving force for Zn to reduce Cu_2O, as ZnO also has a fairly low enthalpy of formation.[11] Figure 3(c) shows the XPS spectra for Zn/Cu_2O junctions. The Cu 2p data shows that Zn, similarly to Zn-rich ZnO, reduces the CuO on the surface. However, the Cu Auger peak shows a second lower binding energy peak indicating Cu is forming at the interface. Therefore, solely by altering the partial pressures of Zn and O_2 during deposition, we were able to create Cu_2O heterointerfaces that were stoichiometric, or had elemental Cu or CuO present at the interface.

3.2 Measurement of Valence Band Offsets

The valence-band offset for the ZnO/Cu_2O heterojunction has been widely studied with published values ranging from 1.7 to 2.8 eV.[17-21] However, little attempt has been made to correlate the observed variation in the offset with deviations in interface stoichiometry. The ZnO/Cu_2O valence-band offsets were determined for the stoichiometric and CuO-containing interfaces via the Kraut method using XPS.[23] In short, the binding energy difference between the Cu 3*s* and Zn 3*s* core-levels was observed for thin ZnO/Cu_2O interfaces. The bulk core-level to valence-band maximum energy differences for Cu_2O and ZnO were determined by fitting the valence-band region of the respective photoelectron spectrum to an instrument-convolved valence-band density of states calculated by density functional theory. The details of this procedure have been reported previously to successfully determine the band alignment of II-VI materials with other earth abundant PV absorbers.[24]

We found the stoichiometric interface and the interface with CuO precipitates had valence-band offsets of 2.4 eV and 2.0 eV respectively, indicating that the presence of a CuO interfacial species changes the band energetics between Cu_2O and ZnO. The two band structures are compared in figure 4. The modification of heterojunction band alignment with the insertion of an interfacial layer has been observed previously in III-V and II-VI material systems.[25] The dependence of the band offset on interface composition, which in turn is dependent on the ZnO deposition conditions, is likely responsible for the large variation in reported offset values and emphasizes the need for improved control and understanding of the interface stoichiometry.

3.3 Performance of Photovoltaic Devices with Different Interface Species

Photovoltaic performance was used to evaluate the relationship between the interface stoichiometry and the electronic quality of ZnO/Cu_2O heterojunctions. Figure 5 displays J-V measurements for devices made with a stoichiometric interface, with CuO at the interface, and with Cu present at the interface. The data was collected under simulated AM1.5 1-sun solar illumination. We focused our analysis on the device open-circuit voltage V_{OC} because it is more sensitive to interfacial and bulk defects and is thus considered an appropriate measure of

interface quality. The reported V_{OC}s were averaged over a minimum of 9 tested devices. The stoichiometric device demonstrated the highest V_{OC} of 530 ± 4 mV. The devices fabricated with CuO and Cu inclusions at the interface had substantially lower average V_{OC}s of 109 ± 11 mV and 347 ± 30 mV, respectively. The short-circuit current densities (J_{SC}) and efficiencies of all of the devices were limited by the resistivity (ρ>1500 Ω-cm) and thickness (~1 mm) of the Cu_2O substrate, and were not as reproducible as device V_{OC}s.

Based solely on the valence-band offset measurements, one would expect the CuO interface to produce the highest V_{OC} because it should have a larger built-in voltage than the stoichiometric interface. However, the opposite trend was observed from the device measurements. There are several possible reasons for this including increased recombination at the interface and Fermi level pinning due to the low band gap of CuO (1.2 eV). However, we believe the lower observed V_{OC} for the device with CuO at the interface is most likely due to the degenerate nature of CuO. It is difficult to make a rectifying contact to CuO, and its presence would likely make contact at the junction nearly ohmic.[26]

Finally, the V_{OC} observed for the Cu interface is in agreement with the expectation that a Cu/Cu_2O Schottky barrier is formed at the interface and the device is therefore limited by the work function difference between Cu_2O and Cu metal.[4, 13] These results show the importance of controlling the emitter deposition conditions in order to control the heterojunction interfacial composition. Clearly, a stoichiometric Cu_2O interface is desirable for obtaining improved PV device performance.

Conclusions

We have demonstrated the ability to tune the Cu oxidation state between CuO, Cu_2O, and Cu at the ZnO/Cu_2O interface with careful modification of the emitter deposition conditions. High-resolution XPS was used to accurately probe the interface stoichiometry as well as the band alignment between the two semiconductors. It was found that the presence of CuO at the interface causes a 0.4 eV shift in the valence-band offset between Cu_2O and ZnO, which could help explain the variance in literature values of the ZnO/Cu_2O valence-band offset. Furthermore, photovoltaic device performance of ZnO/Cu_2O heterojunctions was observed to depend strongly on interfacial composition. Stoichiometric interfaces demonstrated significantly higher V_{OC}s than mixed phase interfaces under AM1.5 1-sun illumination. The control of interfacial chemistry demonstrated herein is directly transferable to other heterojunction systems incorporating a Cu_2O absorber and should result in further improvements in solar conversion efficiency.

Uncategorized References

1. Wadia, C., A.P. Alivisatos, and D.M. Kammen, *Materials availability expands the opportunity for large-scale photovoltaics deployment.* Environ Sci Technol, 2009. **43**(6): p. 2072-7.
2. Olsen, L.C., F.W. Addis, and W. Miller, *Experimental and Theoretical-Studies of Cu2o Solar-Cells.* Solar Cells, 1982. **7**(3): p. 247-279.
3. Rai, B.P., *Cu2o Solar-Cells - a Review.* Solar Cells, 1988. **25**(3): p. 265-272.
4. Assimos, J.A. and D. Trivich, *Photovoltaic Properties and Barrier Heights of Single-Crystal and Polycrystalline Cu2o-Cu Contacts.* Journal of Applied Physics, 1973. **44**(4): p. 1687-1693.
5. Musa, A.O., T. Akomolafe, and M.J. Carter, *Production of cuprous oxide, a solar cell material, by thermal oxidation and a study of its physical and electrical properties.* Solar Energy Materials and Solar Cells, 1998. **51**(3-4): p. 305-316.
6. Weichman, F.L., *Photoconductivity of Cuprous Oxide in Relation to Its Other Semiconducting Properties.* Physical Review, 1960. **117**(4): p. 998-1002.
7. Berezin, A.A. and F.L. Weichman, *Photovoltaic effect in cuprous oxide-copper junctions in relation to the optical absorption spectrum of cuprous oxide.* Solid State Communications, 1981. **37**(2): p. 157-160.
8. Trivich, D., et al., *Cuprous-Oxide Photovoltaic Cells.* Journal of the Electrochemical Society, 1977. **124**(8): p. C318-C318.
9. Minami, T., Y. Nishi, and T. Miyata, *High-Efficiency Cu2O-Based Heterojunction Solar Cells Fabricated Using a Ga2O3 Thin Film as N-Type Layer.* Applied Physics Express, 2013. **6**(4): p. 4.
10. Biccari, F., C. Malerba, and A. Mittiga, *Chlorine doping of Cu_2O.* Solar Energy Materials and Solar Cells, 2010. **94**(11): p. 1947-1952.
11. Chase, M.W.J., *NIST-JANAF Thermochemical Tables*, in *NIST Chemistry WebBook, NIST Standard Reference Database Number 69*. 1998: Gaithersburg MD.
12. Trivich, J.A.A.a.D., *The Photoelectric Threshold, Work Function, and Surface Barrier Potential of Single-Crystal Cuprous Oxide.* Physica Status Solidi (a), 1974. **26**(2): p. 12.
13. Olsen, L.C., R.C. Bohara, and M.W. Urie, *Explanation for the Low Efficiency Cu_2O Schottky Barrier Solar Cells.* Applied Physics Letters, 1979. **34**(1): p. 47-49.
14. Xue, J. and R. Diekmann, *The High-Temperature Phase Diagram of the Cu-O system in the Stability Region of Cuprous Oxide (Cu_2O).* High Temperatures-High Pressures, 1990. **24**: p. 271-284.
15. A. Mittiga, E.S., F. Sarto, M. Tucci, and R. Vasanthi, *Heterojunction Solar Cell with 2% Efficiency Based on a Cu_2O Substrate.* Applied Physics Letters, 2006. **88**(16): p. 2.
16. Minami, T., et al., *High-Efficiency Oxide Solar Cells with ZnO/Cu2O Heterojunction Fabricated on Thermally Oxidized Cu2O Sheets.* Applied Physics Express, 2011. **4**(6): p. 062301.
17. Lee, Y.S., et al., *Ultrathin amorphous zinc-tin-oxide buffer layer for enhancing heterojunction interface quality in metal-oxide solar cells.* Energy & Environmental Science, 2013. **6**(7): p. 2112.
18. Duan, Z., et al., *Effects of Mg composition on open circuit voltage of Cu2O–MgxZn1−xO heterojunction solar cells.* Solar Energy Materials and Solar Cells, 2012. **96**: p. 292-297.
19. Kramm, B., et al., *The band alignment of Cu2O/ZnO and Cu2O/GaN heterostructures.* Applied Physics Letters, 2012. **100**(9): p. 094102.
20. Wong, L.M., et al., *Growth of Cu_2O on Ga-doped ZnO and their interface energy alignment for thin film solar cells.* Journal of Applied Physics, 2010. **108**(3): p. 033702.
21. Ichimura, M. and Y. Song, *Band Alignment at the Cu2O/ZnO Heterojunction.* Japanese Journal of Applied Physics, 2011. **50**(5): p. 051002.
22. Chawla, S.K., N. Sankarraman, and J.H. Payer, *Diagnostic Spectra for Xps Analysis of Cu-O-S-H Compounds.* Journal of Electron Spectroscopy and Related Phenomena, 1992. **61**(1): p. 1-18.

23. Kraut, E., et al., *Semiconductor core-level to valence-band maximum binding-energy differences: Precise determination by x-ray photoelectron spectroscopy.* Physical Review B, 1983. **28**(4): p. 1965-1977.
24. Bosco, J.P., et al., *Band Alignment of Epitaxial ZnS/Zn_3P_2 Heterojunctions.* Journal of Applied Physics, 2012. **112**(9): p. 093703.
25. Franciosi, A. and C.G. VandeWalle, *Heterojunction band offset engineering.* Surface Science Reports, 1996. **25**(1-4): p. 1-+.
26. Wang, P., X. Zhao, and B. Li, *ZnO-coated CuO nanowire arrays: fabrications, optoelectronic properties, and photovoltaic applications.* Opt Express, 2011. **19**(12): p. 11271-9.

Material	Enthalpy of Formation
Cu_2O	-168.6 kJ/mol
CuO	-156.1 kJ/mol
Al_2O_3	-1675.7 kJ/mol
MgO	-601.7 kJ/mol
ZnO	-348.3 kJ/mol
SiO_2	-909.1 kJ/mol

Table 1 Enthalpy of formation for select oxides from NIST.

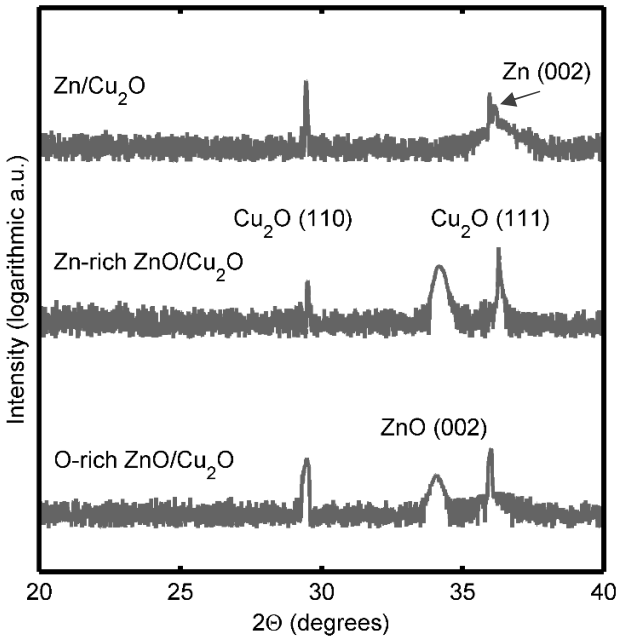

Figure 1 X-Ray diffraction data of Zn and ZnO on Cu_2O indicates ZnO, Zn, and Cu_2O are all phase pure.

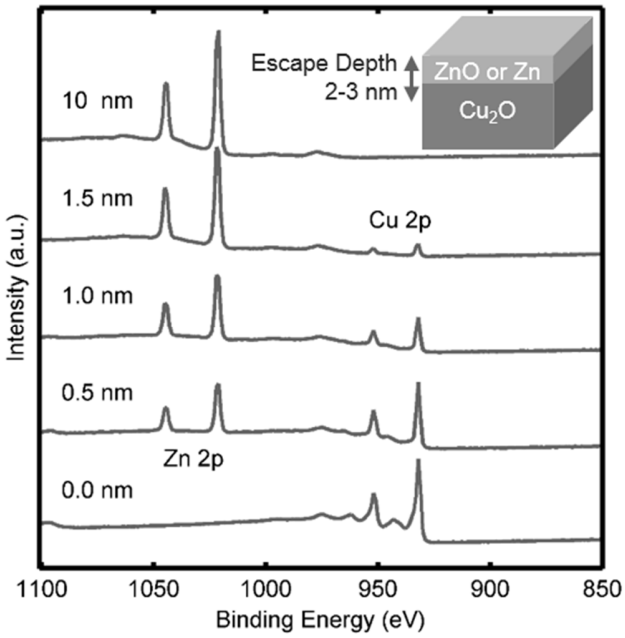

Figure 2 X-Ray photoelectron spectroscopy of Zn-rich ZnO/Cu_2O heterojunctions for indicated thickness of ZnO. Both Cu and Zn peaks are visible meaning the interface is being effectively probed.

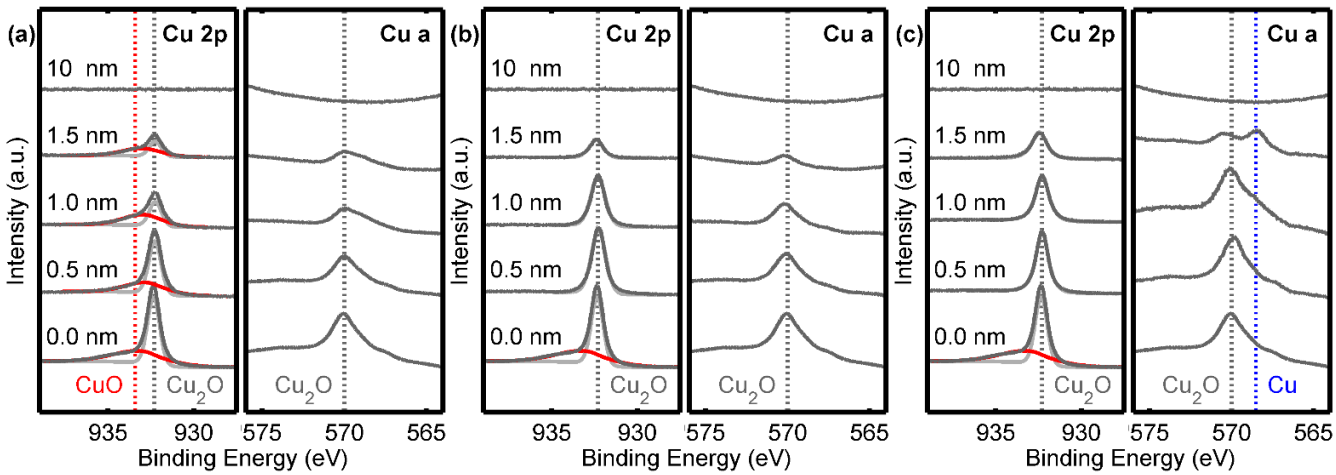

Figure 3 High resolution X-Ray photoelectron spectroscopy of the Cu $2p_{3/2}$ and main Cu Auger peak for Cu_2O heterointerfaces made with (a) O-rich ZnO, (b) Zn-rich ZnO and (c) elemental Zn. The thickness of the deposited ZnO or Zn is indicated. The heterojunctions made with Zn-rich ZnO have a stoichiometric interface while the samples made with O-rich ZnO and Zn have CuO and Cu present, respectively.

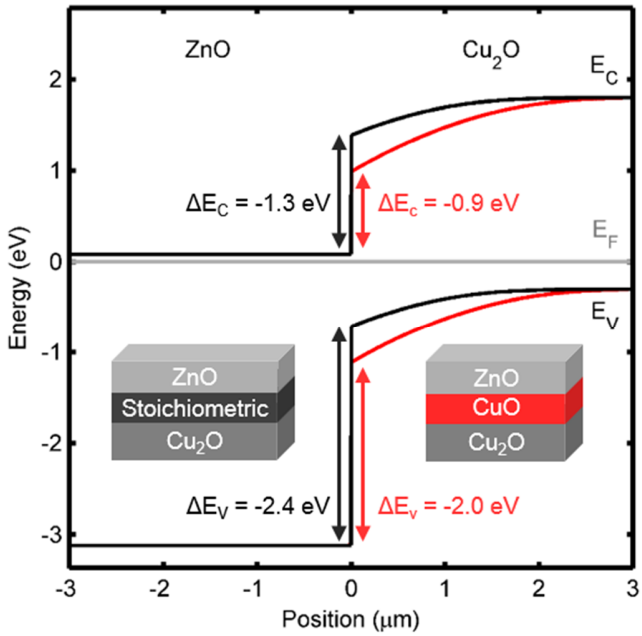

Figure 4 Band structure and valence band offset measurements derived from X-Ray photoelectron spectroscopy measurements of Zn-rich ZnO/Cu_2O (stoichiometric interface) and O-rich ZnO/Cu_2O (CuO at interface) samples.

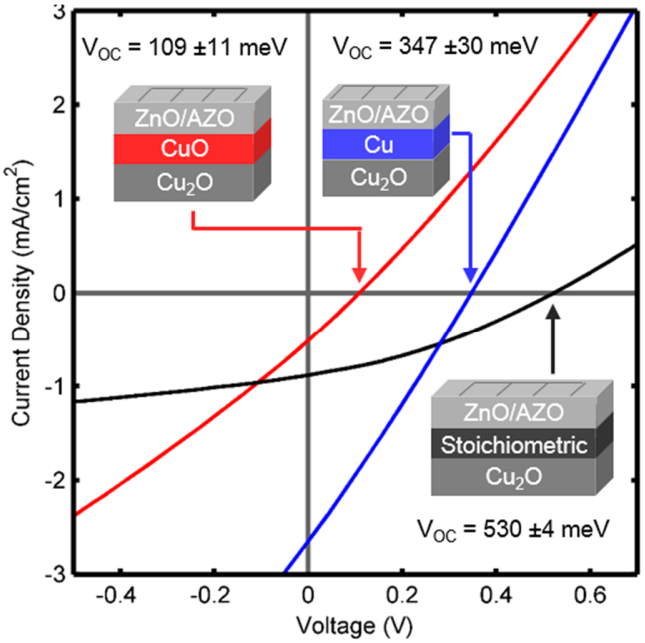

Figure 5 Current density-voltage characteristics for devices made with O-rich ZnO/Cu_2O (CuO at interface), ZnO/Zn/Cu_2O (Cu at interface), and Zn-rich ZnO/Cu_2O (stoichiometric interface).